Hydrodynamic Coefficients of Yawed Square Cylinder in Oscillating Flow

X. Lou, T. Zhou & L. Cheng
School of Civil, Environmental and Mining Engineering, The University of Western Australia, Crawley, Australia

ABSTRACT: This study investigated the effect of yaw angles (α) on the hydrodynamic forces of a square cylinder oscillating in still water. The independent principle (IP), which is generally applicable for the steady current, was examined in oscillating flows. The in-line and transverse forces were measured with a load cell at different Keulegan-Carpenter (KC) numbers and Stokes parameters (β). The normalized drag (C_{DN}) and inertia (C_{MN}) coefficients were evaluated with the least square method by minimizing the difference between measured in-line force and the theoretical value predicted by the Morison equation. The spectrum of lift force and the normalized root-mean-square (C_{LrmsN}) lift coefficients were examined to illustrate the cylinder yaw angle effect. Significant differences are observed for KC in the range of 8~20, where C_{DN} at $\alpha = 45°$ is about 50% higher than that at $\alpha = 0°$, indicating the invalidity of the IP in oscillating flow over this KC number range. The inertia coefficient C_{MN}, however, decreases with the increase of yaw angle, except for KC = 10~18, where a sudden drop of C_{MN} is found to be absent for $\alpha = 45°$ and the magnitude of C_{MN} at $\alpha = 0°$ is the smallest. The high peak on the spectrum of the lift force time series reflects the increase of vortex shedding energy as the yaw angle become larger. In addition, some influences of yaw angles on lift coefficients are also observed despite they are not as significant as that on C_{DN} or C_{MN}.

Keywords: Hydrodynamics, Yawed square cylinder, Oscillating flow

1 INTRODUCTION

Oscillating flows around a cylindrical structure are of theoretical and practical importance due to its intrinsic interest in theoretical hydrodynamic research and relevance to practical engineering applications. Knowledge of environmental hydrodynamics is essential in both the design and operation of offshore structures, such as semisubmersibles and tension leg platforms. For some cylindrical structures, owning to their directionality, the sea waves can approach the structures obliquely. In these cases, the fluid velocity in the axial direction of the structure is not negligible, which may have profound effects on vortex instability, vortex regime classifications and force characteristics. For a yawed circular cylinder, it has been found that over a certain range of yaw angle the normalized Strouhal number ($St_N = f_0 d / U_N$, where f_0 is the vortex shedding frequency, d is the diameter of the cylinder and U_N is the velocity component normal to the cylinder axis) and the normalized drag coefficient ($C_{DN} = F_D / (0.5 \rho U_N^2 d)$, where F_D is the drag force and ρ is the density of the flow), are the same as those when the cylinder encounters a normal incidence flow. This is normally known as the Independence Principle (IP). A number of studies on a yawed circular cylinder have been reported to describe the variation of hydrodynamic coefficients as a function of Keulegan-Carpenter number (KC = $U_m T / D$, where U_m is the maximum velocity of the sinusoidal oscillation) and Stokes number ($\beta = Re / KC$, where Re is Reynolds number).

According to the results from a test with harmonically oscillated flow about a yawed cylinder by Sarpkaya (1982), the independent principle does not apply due to the significant derivation in C_{DN} for the inclined cylinder from the vertical one, except in the high KC drag-dominated range where it may be valid. It is also stated that in waves the independent principle may not apply at all. Cotter and Chakrabarti (1984) measured the oscillatory wave forces on a fixed yawed cylinder at three angles of 0°, 30° and 45°.

They found that the independent principle for the yawed cylinder seems valid if the normal component of the velocity and acceleration are applied in the Morison equation. Therefore, data from the vertical cylinder may be applicable to the yawed cylinder as long as the appropriate form of the Morison equation is applied. However, based on the total force coefficient measurements for inclined circular cylinders, Chakrabarti and Armbrust (1987) pointed out that the large variation in both the drag and inertia coefficients, which indicated the invalidity of IP, are observed for the cylinder inclination angles of 60° to 90° in KC range of 10 to 20 only occurs in an oscillatory flow due to the returning of the vortices shed in the previous cycle to the subsequent cycle. While for waves, the randomness of the wake field and the less dependence on the flow history make the flow more stable and the force coefficients less sensitive to the cylinder yaw angle. Sundar et al. (1998) conducted a test of a cylinder yawed against and along the direction of wave propagation. It was observed that the angle of orientation of the cylinder with the vertical axis has to be considered for the evaluation of wave pressures, especially for KC < 4. The drag coefficient for $\alpha = 45°$ is found to be slightly higher than that for other angles while the inertia coefficient for $\alpha = 0°$ is found to be much higher than that of other angles. Franzini et al. (2009) experimentally investigated the vortex-induced vibration on yawed cylinders which were constrained to oscillate only in the transverse direction. Both the lift and drag coefficients decrease as the yaw angle increases as expected. However, the values of the lift force coefficient for all angles follow a similar behavior in the range of reduced velocity tested when the normal velocity component is considered in the evaluation.

While the flow and hydrodynamic features of a yawed circular cylinder in oscillating flows have been reported extensively, our knowledge about the wake characteristics of a yawed square cylinder in oscillating flows is limited. It has been showed that the sharp corners on the square cylinder may play a significant role in the evolution of flow instabilities and force characteristics in steady flows. In the present study, a square cylinder undergoing forced sinusoidal oscillation in still water was studied at yaw angles of 0°, 15°, 30° and 45°. To investigate the application of IP in the subcritical flow (*Re* = 2700~38000) regime, the in-line and transverse forces were measured with a 3-component force link. The reliability of the present experimental setup has been validated by comparing the measured results on a circular cylinder reported previously.

2 EXPERIMENT SETUP

A schematic diagram of the present experiment is shown in Figure 1. The experiment was conducted in a water flume in School of Civil, Environmental and Mining Engineering, The University of Western Australia. A belt-driven linear actuator (HISAKA) was used to achieve the linear oscillating movement. Two sets of smooth aluminum cylinder tubes with square (side length of 0.04m) and circular (diameter of 0.04m) cross-sections were applied in the experiment. The ends of the cylinders have been sealed properly and cut with their planes being parallel to the flume bottom wall. A gap of 5mm was left between the end of the cylinder and the bottom of the water flume to reduce the end effect. The yawed cylinders were made with the same vertically projected length. The in-line and transverse forces were measured with KISTLER 3-component force link (9317B). A laser displacement sensor was mounted at the end of the actuator to record the displacement of the cylinder instantaneously with the force. The displacement data was used as a reference for later data processing.
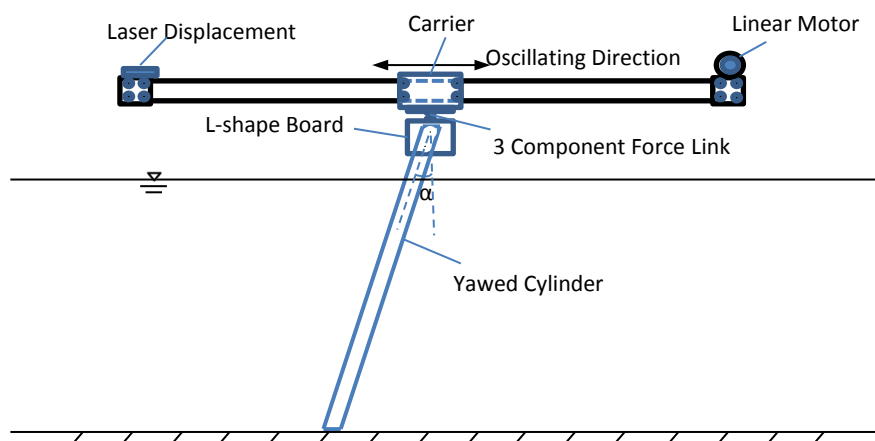

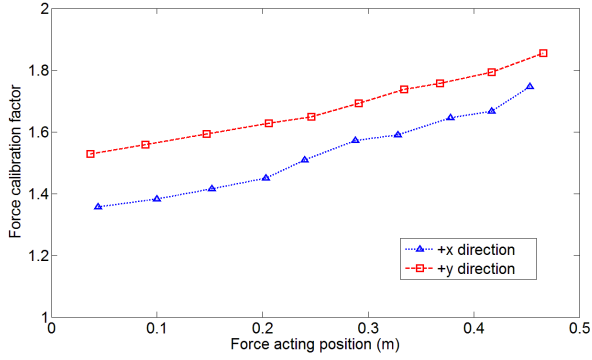Figure 1. Schematic diagram of the experimental setup.

Figure 2. Two typical static calibration curves.

Calibration of the load cell has been done by the manufacture. To avoid the influence of moment due to eccentric force, as well as the water trapped effect, more calibrations are needed before the start of experiment. By placing the model horizontally and hanging some known amount of weight at different locations along the cylinder, the actual weight and the measured weight can be compared and a calibration factor can be found. Extensive static calibration in both the $\pm x$ and $\pm y$ directions indicated that the measured force is practically linearly proportional to the distance between the force acting point and the center of load cell (Figure 2). Considering the resultant force point for water depth of 0.40m, the calibration factors for both in-line and transverse directions were determined. The interval between two consecutive test cases was set to at least 1 minute to make sure the water surface totally level out. The sampling frequency was set at 200Hz. Some noise can be found in the measured signals due to the high sensibility of the load cell, drift of force signals, as well as the mechanical vibration during the oscillation. Filtering and modification have been applied to signals for further processing. Table 1 lists the experimental parameters for the vertical square cylinder ($\alpha = 0°$).

Table 1. Experiment parameter ranges for the square cylinder

Period (s)	Amplitude (m)	U_m (m/s)	KC	Re	β
1.0	0.02~0.15	0.12~0.94	3~24	5000~38000	1600
1.5	0.02~0.18	0.08~0.75	3~28	3400~30000	1067
2.0	0.02~0.20	0.06~0.63	3~31	2500~25000	800
2.5	0.02~0.20	0.05~0.50	3~31	2000~20000	640
3.2	0.04~0.20	0.07~0.39	5~31	2700~16000	500

3 RESULTS AND DISCUSSION

3.1 *In-line force*

In waves and oscillating flows, the total forces can be expressed using Morison Equation:

$$F = C_M \rho \frac{\pi}{4} D^2 \dot{u} ds + C_D \frac{1}{2} \rho D u |u| ds \tag{1}$$

where F is the total in-line force, C_M is the inertia coefficient, C_D is the drag coefficient, D is the diameter of cylinder, u and $\dot{u}$ are the flow velocity and acceleration, ρ is the density of water and ds is the immersed length of the cylinder in water. The first term of the right-hand side of the equation is the inertia force due to the flow acceleration and second term is the drag force related to flow velocity. Here C_M =1+C_A, C_A is the added mass coefficient and 1 accounts for the hydrodynamic force from pressure gradient which is required to accelerate the flow. However, for a cylinder oscillating in still water, the pressure is no longer required and only the added mass is used in Morison Equation:

$$F = C_A \rho \frac{\pi}{4} D^2 \dot{u} ds + C_D \frac{1}{2} \rho D u |u| ds \tag{2}$$

C_M and C_D are calculated from the measured in-line force with least square method. Since the Morison equation describes the in-line force perpendicular to a slender model, the yaw angle effect should be taken into consideration when the cylinder is yawed at a certain angle, the Morison equation may be extended to

$$F = C_A \rho \frac{\pi}{4} D^2 \dot{u}_N ds + C_D \frac{1}{2} \rho D u_N |u_N| ds \tag{3}$$

The subscript N denotes the components of velocity and acceleration which are normal to the axis of the cylinder.

3.1.1 *Data processing*
The time series of the total force recorded from the x-axis direction includes two parts, i.e. the in-line force and the mechanical inertia force of the model. Figure 3 shows an example of raw force data, together with the oscillating motion profile recorded by the laser displacement sensor. An FFT (fast Fourier transform) filter technique is applied to obtain no-phase-shift filtered data. The cutoff frequency is chosen as 4 times of the oscillatory frequency. The inertia force of the model is theoretically calculated from the mass of the model and the acceleration of oscillatory movement. It is subtracted firstly from the total force to get the net in-line force for further data processing. Both the added mass and the drag force coefficients are calculated using least square method. A matlab program based on this method is developed for the drag and inertia coefficients calculation.
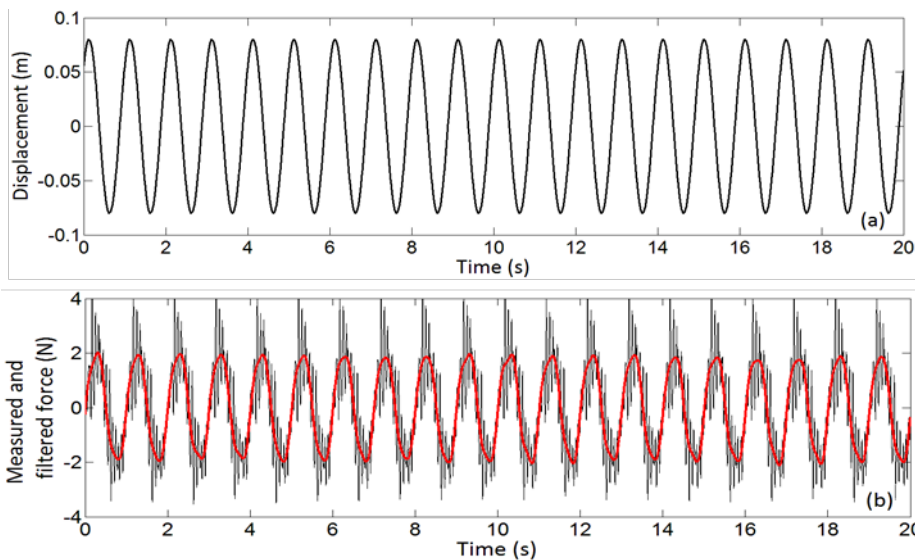

Figure 3. Oscillating motion profile, measured force and filtered force signals at amplitude of 0.08m and period of 1s.
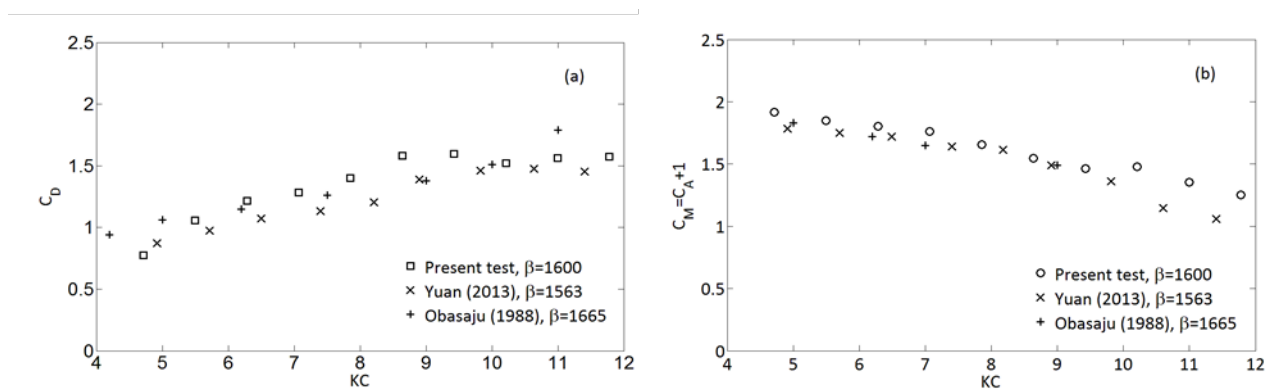

Figure 4. Drag and inertia coefficients of a circular cylinder at $\alpha = 0°$ and $\beta = 1600$.

3.1.2 *Inertia and drag coefficients*
For the convenience of comparison with results reported previously, the inertia coefficient will be shown here instead of added mass coefficient. To validate the experimental setup, tests were first conducted for a circular cylinder model in oscillating flows at $\alpha = 0°$ due to the availability of the C_D and C_M results over a large range of KC numbers. Both the inertia and drag force coefficients of a circular cylinder for

228

different KC numbers at β = 1600 are presented in Figure 4, and compared with previously published re-
sults. Considering the large uncertainty of force measurements in oscillatory flows, the two hydrodynamic
coefficients show very well agreement with the other experimental results at approximately the same β
numbers (Obasaju et al., 1988; Yuan, 2013), validating the present experiments. Some small discrepan-
cies, however, are inevitable due to the different experimental setup and experimental uncertainties. For
the cases with apparent discrepancies, tests were repeated several times to eliminate the probability of ex-
periment errors and minimize the relative uncertainties to less than 5%.

The drag coefficients of the square cylinder at different yaw angles are shown in Figure 5. Only the re-
sults at β = 1067 are demonstrated here due to the similar features and the limitation of the paper length.
Generally, C_{DN} decreases with KC number for α = 0°. When KC becomes large enough, C_{DN} ap-
proaches gradually to approximately 1.8, where the flow is considered as quasi-steady flow and the drag
coefficient tends to the value in steady currents (Laya et al., 1984). Sumer and Fredsoe (2006) suggested
that the transverse vortex street will disappear and the shedding vortices will form a vortex street parallel
to the oscillatory direction as KC is increased beyond 13, in much the same way as in the steady current.
When the cylinder is inclined to the flow, a significant difference can be observed in the drag coefficients
for different yaw angles when KC ≤ 5 in that C_{DN} at α = 45° is larger than that of other angles, which
corresponds well with the results of the yawed circular cylinder by Sundar et al. (1998). For KC in the
range of about 8 and 20, there is a dramatic deviation of C_{DN} at α = 30° and 45° from that of other an-
gles. Specifically, C_{DN} almost keeps constant for α = 0° and 15°, and increases as α = 30° and 45°.
Particularly the difference of C_{DN} between α = 0° and 45° can be more than 50% at some KC numbers
and is too big to attribute to the experimental uncertainties. The present results are similar to that of a cir-
cular cylinder from Sarpkaya et al. (1982), who found the significant increase in C_{DN} is absent for yawed
cylinders for KC in the range of 8 to 25, showing a trend of decrease in the magnitude of C_{DN} for α =
45°. This result indicates the invalidation of IP in the oscillating flow over this KC range.
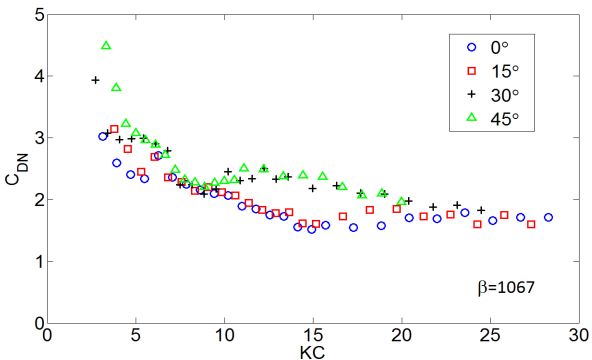

Figure 5. Drag coefficients of yawed square cylinder for different KC numbers at β = 1067.

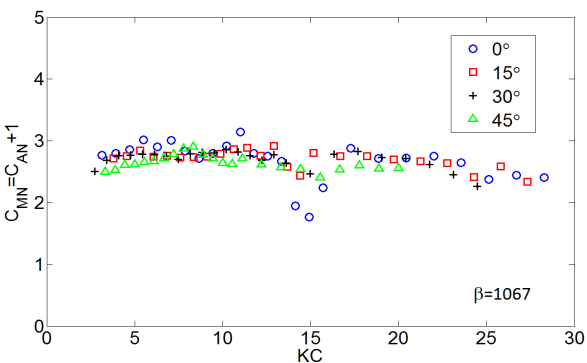Figure 6. Inertia coefficients of yawed square cylinder for different KC numbers at β = 1067.

With regard to a circular cylinder, a negative value of C_A ($C_M < 1$) has been found around $10 \leq KC \leq$
18 for some β numbers, which commonly referred as the 'inertia crises' (Sumer and Fredsoe, 2006). For
the inertia coefficient C_M of a square cylinder (Figure 6), a sudden drop in C_M can also be observed at
around KC = 12~18 for all the angles. The largest difference in C_{MN} between the yawed cylinder and
the vertical one is also observed over this KC range (Figure 6). Within this range, C_{MN} increases signifi-
cantly as α increases, especially for α = 45°. The variation of C_{MN} in the whole measured KC range
demonstrates a level trend without trough, which is in accordance with the yawed circular cylinder results

from Sarpkaya et al. (1982) and Garrison (1985). For KC $\leq$ 12 and KC $\geq$ 18, the difference in the results of C_{MN} for all angles is rather small, though a decrease of C_{MN} can be observed as α increases. Some factors may contribute to the apparent difference in the force coefficients between different yaw angles in oscillating flows. According to Chakrabarti and Armbrust (1987), the sweeping back of vortices from the earlier cycle into the subsequent cycle tends to influence the forces on the cylinder. The randomness of vortex generation and the less dependence on the history flow of wake field, on the other hand, makes the oscillatory flow more sensitive to the cylinder angle.

3.2 *Transverse force*

The transverse force, or lift force, undergoes a periodic change as the vortex shedding progresses when a cylinder oscillates in water. The measurement of lift force was conducted simultaneously with the in-line force. A better comprehension of the hydrodynamics around a sinusoidal oscillating yawed cylinder can be gained by examining the spectra and the root-mean-square (RMS) coefficient of lift force. The power spectrum of the lift force data is obtained from FFT method. The dominant frequency can be identified as the fundamental lift frequency normalized by the oscillatory flow frequency which is defined as

$$N_L = f_L/f_O \tag{4}$$

namely the number of oscillations in the lift per flow cycle. The RMS lift force coefficient (C_{Lrms}) is the normalized RMS value of the measured lift force

$$C_{Lrms} = F_{Lrms}/\frac{1}{2}\rho D U_m^2 L \tag{5}$$

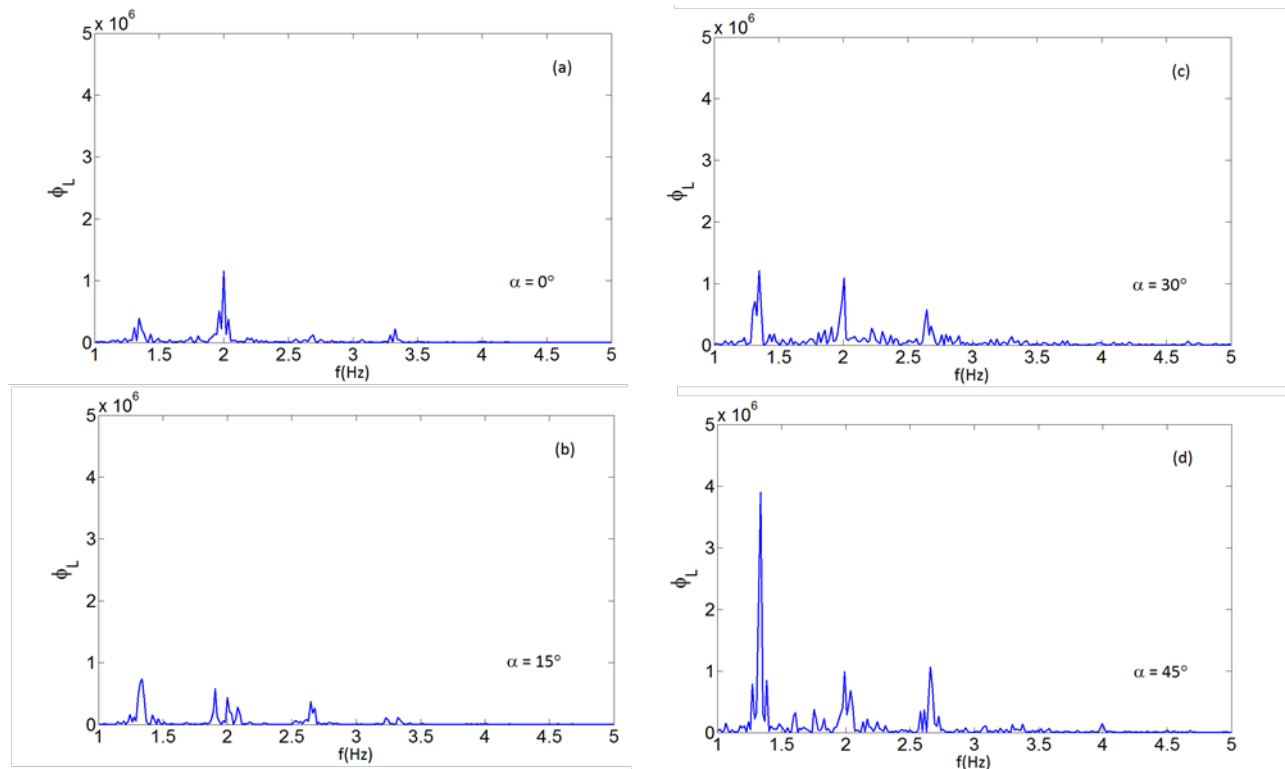where F_{Lrms} is the RMS value of measured lift force.

Figure 7. Spectra of lift force for different yaw angles at KC $= 17.3$ and $\beta = 1067$.

3.2.1 *Dominant lift frequency*
Figure 7 demonstrates the spectra of the lift force of the yawed cylinder at KC $= 17.3$ for $\beta = 1067$. As the peak energy represents the vortex shedding energy, the increase of the magnitude of the peak indicates that the yawed angle has an increasing effect on the flow structure around the cylinder. Though the existence of yaw angle strengths the peak of the spectrum, the vortex shedding frequency f_L, derived from the most pronounced peaks on the spectra, keeps almost constant with 1.34Hz, 1.34Hz, 1.33Hz and 1.32Hz for $\alpha = 0°$, 15°, 30° and 45°, respectively. Considering the oscillating frequency $f_O = 0.67$Hz, the dominant lift frequencies N_L are found to be around 2 for all the yaw angles. This result indicates a flow regime of single pair vortex according to Williamson (1985). However, the double pairs vortex flow regime

should be expected within $15 \leq KC \leq 24$, the delay of the appearance of the double pairs vortex may be attributed to the different Re numbers as well as the fact that it is difficult to define the flow regime rigidly during the transition range of KC. Especially for the lift force spectrum at $\alpha = 0°$, $15°$ and $30°$, a second pronounced peak at $f = 2Hz$ can also be found, probably denoting a dominant frequency of 3 and corresponding to a double pairs vortex flow regime. As mentioned above, for the KC numbers close to the transition range, the flow regime will undergo a transition period as well. Considering the different experiment setup and experiment errors, our results are in good agreement with the previous publications. The normalized shedding frequency, Strouhal number St ($= f_L D/u_N$), was calculated to illustrate the yaw angle effect on the vortex shedding frequency. The values of St are 0.117, 0.119, 0.114 and 0.110 for α of $0°$, $15°$, $30°$ and $45°$, respectively; denoting the validity of IP over the tested yaw angles, at least in terms of vortex shedding frequency.

3.2.2 RMS lift coefficient

The time series of lift force data is examined before further calculation of the lift coefficients. Figure 8 shows the lift force series of the vertical square cylinder with time normalized by the oscillating period for $KC = 17.3$ at $\beta = 1067$. The relation between the lift force time series and the corresponding spectrum is obvious. The number of lift force cycles within one oscillatory period represents the normalized fundamental lift frequency, i.e., 2 cycles of lift force were observed within 1 period as shown in Figure 8. Therefore, $N_L = 2$ can be found in Figure 7 correspondingly, indicating the flow regime of one pair vortex shedding.
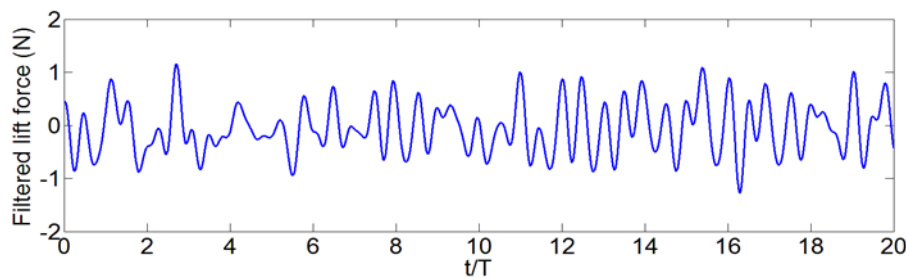

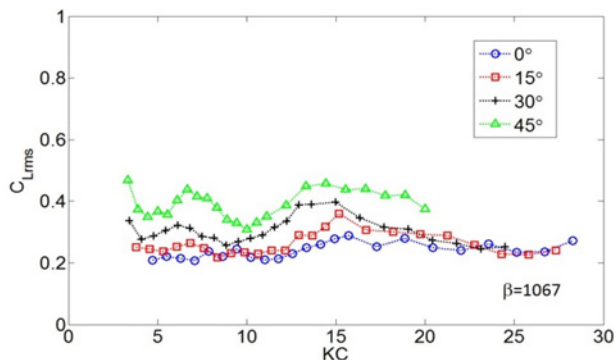Figure 8. Filtered lift force signal at amplitude of 0.11m and period of 1.5s.

Figure 9. Root mean square values of lift force coefficient at different yaw angles.

The results of C_{Lrms} for different yaw angles are shown in Figure 9 as a function of KC number at $\beta = 1067$. For $\alpha = 0°$, two local maxima at KC= 8 and 16, respectively, are observed even though the first one is not as apparent as the second one. This result corresponds well with that from a yaw circular cylinder, of which two local peaks on the C_{Lrms} distribution are observed at about $KC = 10$ and $KC = 17$ for all β numbers (Obasaju et al., 1988). As Williamson (1985) concluded, a new vortex shedding pattern will emerge every time the oscillation amplitude increases by a step that makes KC increase by about 6.75, if the longitudinal distance between two vortices with the same sign in the steady flow is assumed to be approximately the same to oscillatory flow. Considering the yaw angles, the magnitude of C_{Lrms} increases significantly with α. For example, the magnitudes of C_{Lrms} at $\alpha = 30°$ and $45°$ are about 50% and 100% higher than that at $\alpha = 0°$. The results shown in Figure 9 clearly indicate that the IP is not valid for evaluating the lift coefficient on a square cylinder in oscillating flows. The increase in C_{Lrms} may be associated with the feature of the lift force spectrum (Figure 8). As the lift force is due to the asymmetrical vortex patterns, C_{Lrms} is closely related to the vortex shedding and the motion history, manifesting

that the existence of the yaw angle may have an increasing effect on the vortex shedding process. Attentions should also be drawn to the advanced appearance of the local maxima on the C_{Lrms} distribution when α increases. As the KC number is determined by the component of maximum oscillating velocity normal to the cylinder axis, for a certain KC the larger oscillating amplitude should be expected for the cylinder with larger yaw angles. Therefore, the larger oscillating amplitude may induce the corresponding vortex shedding regime.

4 CONCLUSIONS

A well-controlled experimental investigation has been conducted on a square cylinder in terms of the hydrodynamic forces in oscillating flows. The effect of the cylinder yaw angles on the hydrodynamics has been examined. Quantitative comparisons were made between the square cylinder and the circular cylinder to demonstrate the similarities and differences between the two types of cylinders. The main conclusions are summarized below:

The magnitude of C_{DN} increases as the yaw angle increases for the square cylinder, which is opposite to that of the yawed circular cylinder. However, for both kinds of cylinders, the most significant difference among yaw angles are observed in the range KC = 8~20, indicating the invalid of IP in oscillating flows over this KC number range.

The inertia coefficient C_{MN}, decreases with the increase of the yaw angle. Except in the range of KC = 10~18, where a sudden drop of C_{MN} is absent for $\alpha = 45°$ and the magnitude of C_{MN} at $\alpha = 0°$ is the smallest. Similar to the circular cylinder results, the deviation of C_{DN} and C_{MN} observed at different angles in the range KC = 8~20 is attributed to the disruption of the transverse vortex street.

Unlike the results of yawed circular cylinder, from which a reduction of the vorticity structure due to the yaw angle was found, the increase of α may intensify the vortex shedding process behind a yawed square cylinder. This is verified by the increase of the peak energy on the lift force spectra as the yaw angle increases. As C_{Lrms} is also closely related to the vortex shedding and the motion history, the increasing trend corresponds well to the intensified peak energy of the lift force spectra as the yaw angle increases.

REFERENCES

Chakrabarti, S.K., Armbrust, S.F. (1987). Total Force Coefficients for Inclined Cylinders. J Waterway, Port, Coastal and Ocean Engineering, Vol 113, pp. 421-426.
Cotter, D., Chakrabarti, S. (1984). Wave Force Tests on Vertical and Inclined Cylinders. J Waterway, Port, Coastal and Ocean Engineering, No. 110, pp.1-14.
Franzini, G.R., Fujarra, A.L.C., Meneghini, J.R. (2009). Experimental Investigation of Vortex-Induced Vibration on Rigid, Smooth and Inclined Cylinders. J Fluids and Structures, Vol 25, pp. 742-750.
Garrison, C.J. (1985). Comments on Cross-Flow Principle and Morison's Equation. J Waterway, Port, Coastal and Ocean Engineering, Vol 111, pp. 1075-1079.
Laya, E.J., Connor, J.J., Sunder, S.S. (1984). Hydrodynamic Forces on Flexible Offshore Structures. J Engineering Mechanics, Vol 110, pp. 433-448.
Obasaju, E.D., Bearman, P.W., Graham, J.M.R. (1988). A Study of Forces, Circulation and Vortex Patterns around a Circular Cylinder in Oscillating Flow. J Fluid Mech, Vol 196, pp. 467-494.
Sarpkaya, T. (1982). Wave Forces on Inclined Smooth and Rough Circular Cylinders. 14th Annual Offshore Technology Conference, Houston, Texas, OTC4227.
Sumer, B.M., Fredsoe, J. (2006). Hydrodynamics around Cylindrical Structures. World Scientific Publishing Co. Pte. Ltd, Singapore.
Sundar, V., Vengatesan, V., Anandkumar, G., Schlenkhoff, A. (1998). Hydrodynamic Coefficients for Inclined Cylinders. Ocean Engineering, Vol 25, pp. 277-294.
Williamson, C.H.K. (1985). Sinusoidal Flow Relative to Circular Cylinders. J Fluid Mech, Vol 155, pp. 141-174.
Yuan, Z. (2013). Experimental Study of Hydrodynamic Forces on a Surging Circular Cylinder in Still Water and in Regular Waves. Doctor of Philosophy Thesis, Nanyang Technological University, Singapore.